A Dual-Band Dual-Polarized Antenna Design for a Weather Radar with Characteristic Modes Analysis and MoM

Guillermo D. Rodriguez
Departamento de Electrónica
Facultad de Ciencias Astronómicas y Geofísicas de la Universidad Nacional de La Plata
La Plata, Argentina
grodriguez@fcaglp.unlp.edu.ar

Juan Pablo Ciafardini
Departamento de Electrotecnia
Facultad de Ingenieria de la Universidad Nacional de La Plata
La Plata, Argentina
jpciafardini@fcaglp.unlp.edu.ar

R. Ezequiel Garcia
Departamento de Electrónica
Facultad de Ciencias Astronómicas y Geofísicas de la Universidad Nacional de La Plata
La Plata, Argentina
regarcia@fcaglp.unlp.edu.ar

Miguel Ferrando Bataller
Instituto de Telecomunicaciones y Aplic. Multimedia
Universidad Politécnica de Valencia
Valencia, Spain
mferrand@dcom.upv.es

***Abstract*— We describe here an antenna design to be used in a weather Radar for hydrometeors detection and characterization. This antenna could operate in two frequency bands and with any polarization. The proposed model was analyzed and optimized using two simulation methods: Characteristic Modes and Method of Moments..**

Keywords— Weather Radar, Dual-band Dual-polarized Antenna, Characteristics Modes.

I. INTRODUCTION

The use of polarimetry in weather radars allows obtaining more detailed characteristics of the hydrometeors that are the object of the study. The use of two linear polarizations or, sometimes, circular polarization, allows us to obtain the radar cross section for two orthogonal axes, giving data related to the size and sort of hydrometeor on the radar scope. On the other hand, the latest developments are focused on the use of antenna arrays instead of parabolical antennas, employing circular or several faces of planar arrays [1][2][3][4].

Related to the frequencies used, the International Telecommunications Union (ITU), assigned three frequency bands to use with weather radars which are shown in Table I [5].

In terms of the frequency range, we have a compromise between scope and resolution. The lower the frequency (S-band), the better the scope and the worst the resolution as well as larger antennas.

These considerations make that today to be common the use of C and X bands in weather radars that, operating in networks, give enough scope and resolution for most needs.

TABLE I. FREQUENCY BANDS FOR METEOROLOGICAL RADAR BY ITU

Frequency Band	***S***	***C***	***X***
Maximum frequency [GHz]	2.7	5.25	9.3
Minimum frequency [GHz]	2.9	5.75	9.5

With these ideas in mind, we study several antenna geometries, selecting a basic structure with a high bandwidth needed to cover both transmission bands (C and X) and thinking of creating a selective frequency coupling method. The selected model is based on the work of Peñafiel Ojeda et al and Martens et al [6][7][8], and we reach a final model by adding structures to give more bandwidth to the design.

Finally, we present here the development of an antenna that can be used as a unitary element in an array or as a feeder in a reflector antenna. This development could operate with two linear orthogonal polarization or circular polarization. And it is also capable to operate in two frequencies, C-band and X-band to obtain both characteristics, scope, and resolution with a unique antenna.

Are presented electromagnetic simulations of the model made with the software FEKO (Altair), using two methodologies: Method of Moments (MoM) and Characteristic Modes Analysis (CMA). A prototype of the model is starting to be manufactured to validate these simulations.

II. DUAL-BAND DUAL-POLARIZED ANTENNA

The basic structure proposed is showed in Fig. 1 and is formed by a bowl with a mushroom at the center. The dimensions are detailed in Fig. 2 and Table II.

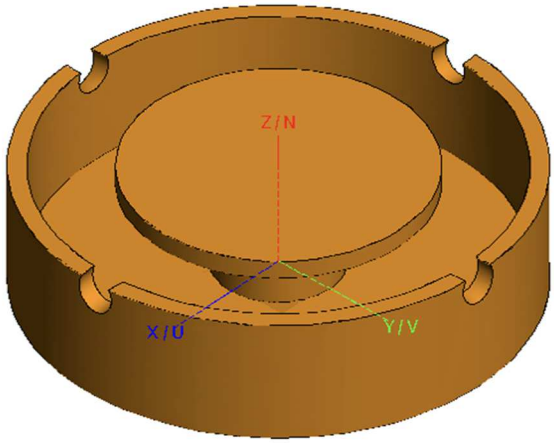

Fig.1 - Dual-Band Dual-Polarized Antenna structure prototype.

TABLE II. DUAL BAND – DUAL POLARIZED ANTENNA STRUCTURE DIMENSIONS.

Parameter	D_e	D_c	D_i	E	H_1
Size [mm]	27.5	3.5	16.5	1.0	5.9

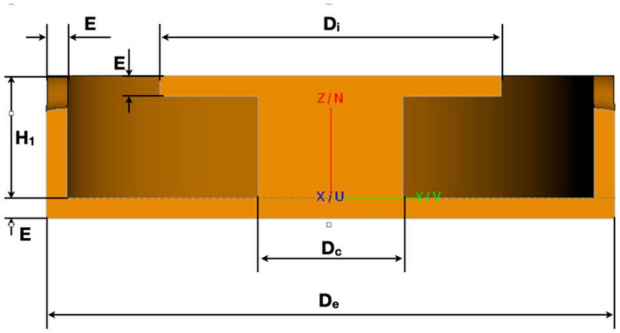

Fig. 2 - Dual-Band Dual-Polarized Antenna structure dimensions.

III. CHARACTERISTIC MODES THEORY

The theory of characteristic modes has a first proposal in [9] and a more elaborated versions in [10][11]. This technique, as an antenna design tool, can provide direct insights into the radiating phenomena on the model and allows the designer to develop antennas more systematically in place of a brute-force approach.

These insights aid in the choice of the basic structure and excitation location for the antenna [12][13] and the use of numeric methods, usually implemented in software tools, help definitively in the task of define the final model [14][15]. As is explained in [16], CMA enables the understanding of the radiation of the proposed model with enough accuracy and in combination with MoM, gives a real insight into develop the feeding techniques.

In CMA, J_i are real currents obtained for each resonance mode i of the model and must be obtained for each frequency of interest. This can be accomplished with MoM, using the generalized impedance matrix of the antenna. As is explained in [10][17]:

$$J = \sum_n \frac{V_n^i J_n}{1 + j\lambda_n} \tag{1}$$

Where J_n are the Eigen-currents, λ_n are the Eigen-values and V_n^i is the modal excitation coefficient.

The modal excitation coefficient can be obtained as:

$$V_n^i = \left\langle J_n, E^i \right\rangle = \iint_S J_n \cdot E^i dS \tag{2}$$

In (1), the product $V_n^i J_n$ shapes the coupling between the excitation and the nth mode, and determines which modes will be excited.

The modal significance, MS_n, is calculated as follows [10]:

$$MS_n = \left| \frac{1}{1 + j\lambda_n} \right| \tag{3}$$

The modal significance take values between $0 < MS_n \leq 1$. When a mode is at resonance, its modal significance, $MS_n = 1$.

The useful bandwidth of a mode BW_n is defined, as usual, related to the power radiated at resonance and is the frequency range in which the power down 3 dB from this value (half power), or, in times, $0.707 \leq MS_n \leq 1$ [18].

Another way to obtain the same data (radiating bandwidth and resonance frequency), is using the characteristic angle, given by (4). In terms of physics, this shape the relative phase between J_n and E_n [16], that is 180º at resonance.

$$\alpha_n = 180^\circ - \tan^{-1}(\lambda_n) \tag{4}$$

In terms of characteristic angles, when the modal significance MS_n reach values of 0.707, the characteristic angles values are 135º or 225º. Then the radiant bandwidth (BW_n) is the range of frequencies for which $135° \leq \alpha_n \leq 225°$ [18].

Therefore, the analyzed model will be a good antenna when the characteristic angle was near 180º.

IV. CHARACTERISTIC MODES ANTENNA ANALYSIS

Here we perform the analysis of the antenna structure shown in Fig. 1, using CM. In Fig.3 we show the normalized current distribution at first resonance for the first six characteristic modes, *Jn*, for this model. These characteristic currents have been obtained with FEKO [18] by using the Characteristic Modes request. Indeed, it represented how is the current flow with red arrows.

Fig. 4 shows the response of modal significance (MSn) with frequency for several current modes Jn. We can identify the more effective radiating modes when MSn is closer to the maximum value.

Therefore, in Fig. 4 it can be seen that mode J_0 resonates at 11.35 GHz, the modes J_1 and J_1' resonate at 6.8 GHz, as indicated by their corresponding modal significance curves, the mode J_2 resonates at 4.7 GHz and the higher-order modes resonate outside the range of frequencies analyzed.

The J_1 and J_1' modes are called degenerate modes as they resonate at the same frequency due to the symmetry of the structure analyzed, and so do the J_3 and J_3' modes.

If the modal significance curves corresponding to the degenerate modes are observed can be seen that are the same and are superposed. Note that J_0 and J_2 have no degenerated modes.

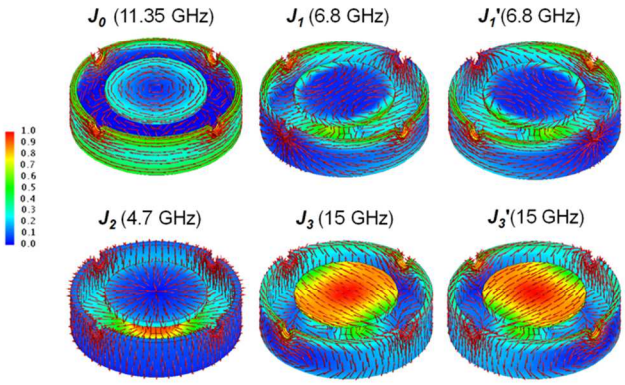

Fig.3 - Normalized current distribution of the first six characteristic modes of the antenna.

In Fig. 5, we can see the characteristic angles (α_n) frequency response for several current modes J_n. As we mentioned, the resonance of the modes occurs for characteristic angles (α_n) of 180°. There, we can note that there are degenerate modes that are superimposed on the originals (J_1 with J_1' and J_3 with J_3').

Observing the curves of Characteristic Angle (Fig. 5) and Modal Significance (Fig. 4), it can be seen that J_0 is a broadband non-degenerate mode; the curves corresponding to J_0 enter the radiation zone at the frequency corresponding to 7.25 GHz and remain there beyond the analyzed frequency range. In contrast, the J_2 mode is a non-degenerate narrowband mode. The Modal Significance and Characteristic Angle curves remain in the radiation zone only for the frequency range from 4.53 GHz to 4.9 GHz.

The degenerate modes J_1 and J_1' present a case of particular interest, since their currents are orthogonal (see Fig. 3) and can be conveniently excited to generate radiation with orthogonal linear polarizations, or circular polarization[12][16][18][19].

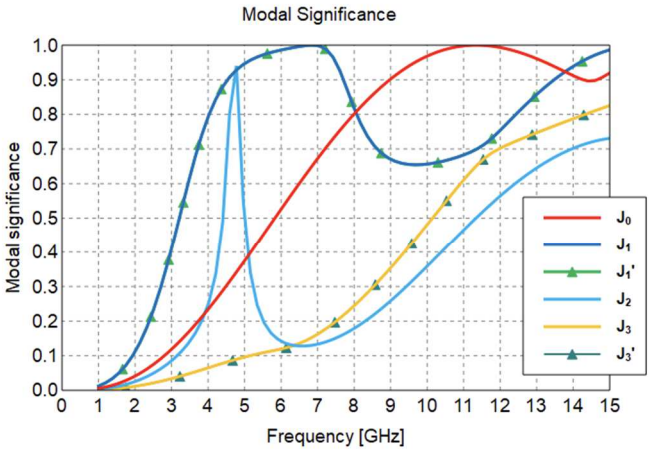

Fig. 4 - Modal significance versus frequency for the first six modes of the antenna.

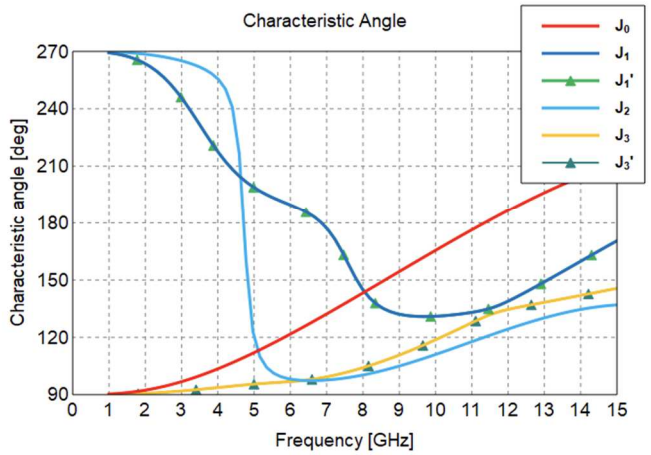

Fig.5 - Characteristic angle versus frequency for the first six modes of the antenna.

In addition, analyzing the curves of Modal Significance and Characteristic Angle we can see that the curves corresponding to these modes enter the radiation zone at the frequency of 3.73 GHz, they remain slightly outside the radiation zone in the frequency range of 8.6 GHz and 11.45 GHz and re-enter the radiation zone for frequencies greater than 11.45 GHz, in the rest of the analyzed frequency range. For practical purposes, it can be considered that modes J_1 and J_1' will present good radiation characteristics for frequencies between 3.73 GHz and higher than 15 GHz, behaving as a mode with ultra-wide bandwidth.

V. ANTENNA FEEDS DESIGN

For the design of the feeds, we could use either inductive or capacitive coupling mechanisms to excite characteristic modes. As a rule of thumb, we will use inductive feeding to excite modes whose electric current distribution with a maximum at the location of the source and a capacitive coupling mechanism to excite modes whose electric field distribution with a maximum at the location of the source.

The design objective sought is to make the antenna work in the frequencies corresponding to the C and X bands assigned to meteorological radars, for this reason, we analyze the current distribution of modes J_1 and J_1' for these

frequencies. In Fig. 6 the normalized current distribution of the modes J_1 and J_1', evaluated at the frequencies of interest are shown.

As can be seen in Fig. 6, modes J_1 and J_1' present a current minimum for both analyzed frequencies at the nodes where the current flow begins and ends on the central disc of the structure. In this way, a capacitive coupling method could efficiently feed the current modes J_1 and J_1' at these points. Based on this analysis, a feeding scheme like the one shown in Fig. 7 was proposed.

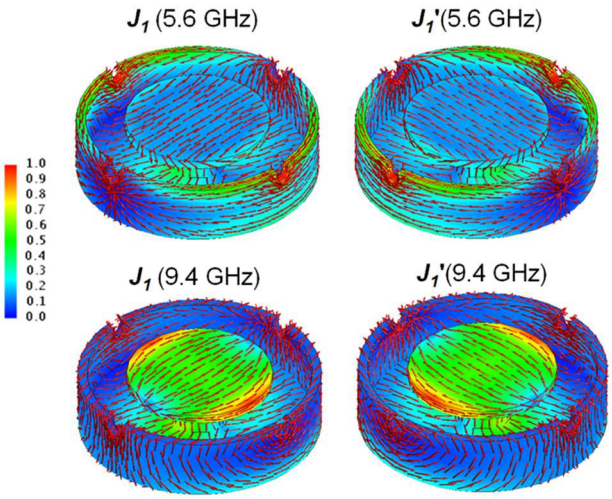

Fig. 6 - Normalized current distribution of the modes J_1 and J_1', evaluated at the frequencies of interest.

For the exciters, we employ capacitive feeders. Instead of the reference design [6], we need a response with passing gaps at two frequencies. For that, we analyze individual geometries for each case, create a dual structure on the base of that case and optimize the structure to obtain good S_{11} characteristics at the desired bands. The feeders' sizes are detailed in Fig. 8, Fig. 9, and Table III.

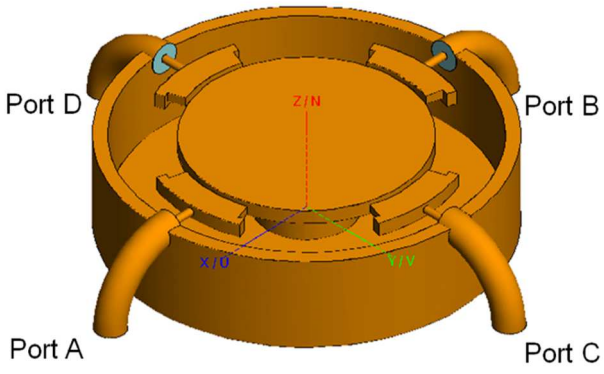

Fig 7 - Antenna feed ports.

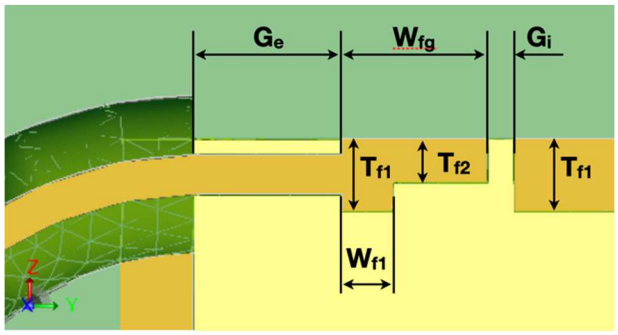

Fig. 8 - Antenna feed ports details, side view.

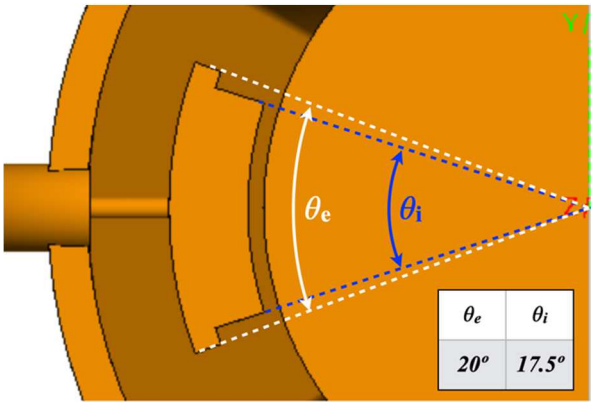

Fig. 9 - Antenna feed ports details, top view.

TABLE III. FEED PORT DIMENSIONS.

Parameter	G_e	G_i	T_{f1}	T_{f2}	W_{f1}	W_{fg}
Size [mm]	2	0.4	1	0.6	0.7	2

In the case of the feed given to the antenna, described above, the modes J_1 and J_1' can be excited effectively since these modes have a minimum current at the feed point, as seen in Fig. 6. Connecting a voltage source between ports A and B of Fig. 7, J_1 mode can be fed, and connecting a voltage source between ports C and D, J_1' mode can be excited.

VI. RESULTS

A. Impedance of ports

The dimensions of the antenna were optimized using MoM to achieve the best impedance matching for the C and X bands, as shown in Fig. 10. This Fig. depicts the simulated reflection coefficient for ports A and B connected with voltage sources with angles of 0° and 180° respectively, and with ports C and D loaded with 50 Ω. As observed, a bandwidth from 5.4 GHz to 5.8 GHz is obtained for S_{11}< -10 dB in the C band and a bandwidth from 9.2 GHz to 9.6 GHz is obtained for S_{11}< -10 dB in the X band.

B. Radiation Pattern

Once this objective was achieved, simulations with MoM were carried out to obtain the radiation pattern of the antenna for the two frequency bands.

Fig. 11 shows the far-field radiation pattern, plotted in three dimensions, for the C band (5.6 GHz) and the X band

(9.4 GHz). The pattern presents good symmetry concerning the vertical of the antenna.

Fig. 12 shows a 2D section of the radiation pattern. The diagram corresponding to band C is shown in blue and the diagram corresponding to Band X is shown in green. For band C, a gain of 6.5 dBi is obtained, and a beamwidth of 90.5°. For the X band, a gain of 9.5 dBi is obtained, and a beamwidth of 53.5°.

C. Polarization

Polarization of the radiation depends on the form in which the antenna it's feed. Feeding ports A and B with voltage sources with phases of 0° and 180° respectively, linear polarization is obtained.

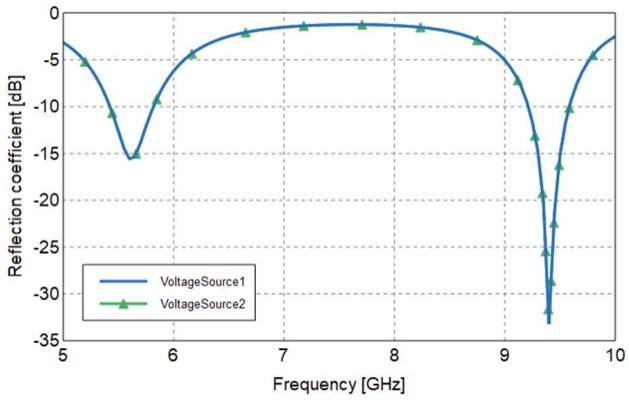

Fig. 10 - Simulated reflection coefficient for the feeding ports of the antenna.

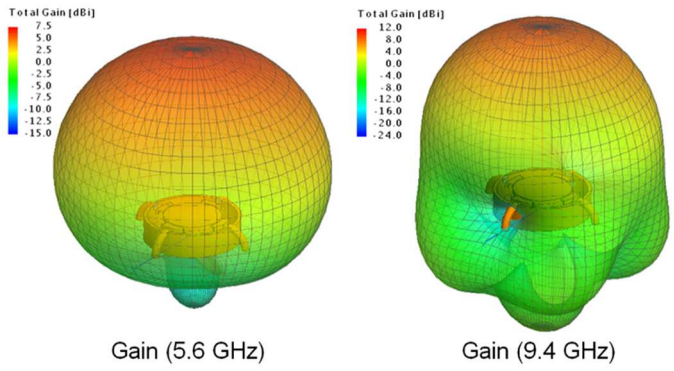

Fig. 11 - 3D Radiation patterns obtained from simulations.

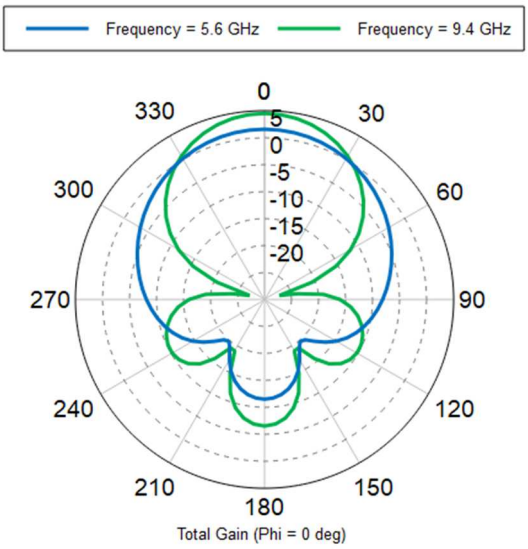

Fig. 12 - 2D Radiation patterns obtained from simulations.

Feeding ports C and D with voltage sources with phases of 0° and 180° respectively, linear polarization orthogonal to the previous case is obtained. Finally, feeding ports A, B, C, and D with voltage sources with a progressive phase of 0°, 90°, 180°, and 270° respectively, circular polarization is obtained.

In a general way, Fig. 13 shows the polarization characterization made by simulations for linear polarization, exciting ports A and B, and matching ports C and D, at 9.4 GHz. For both design frequencies and worst cases, more detailed information about the isolation between co and cross-polarization is presented in Fig. 14 and Fig. 15. Here we are using the third definition of Co and Cross Polarization as defined by Ludwig [20].

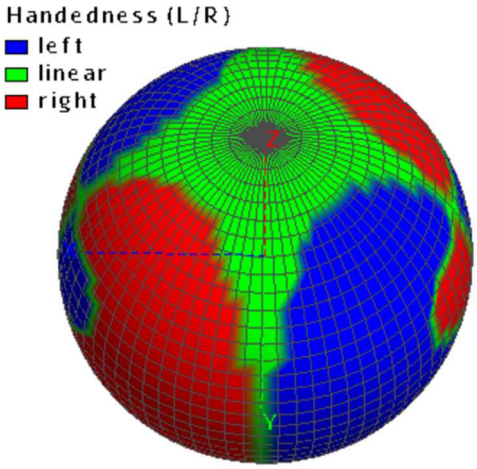

Fig. 13 - Polarization characteristics.

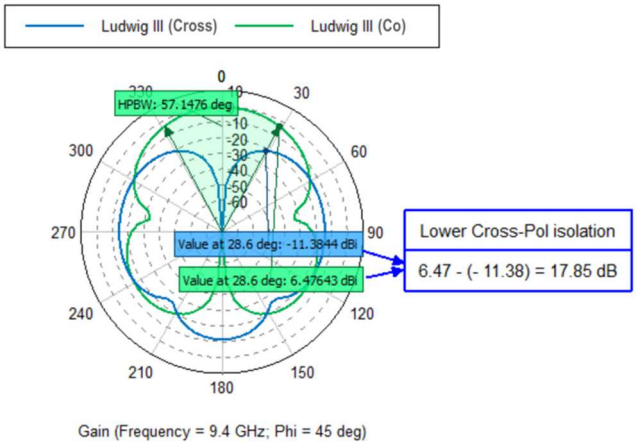

Fig. 14 - Isolation between co and cross-polarization (Freq.: 9.4 GHz).

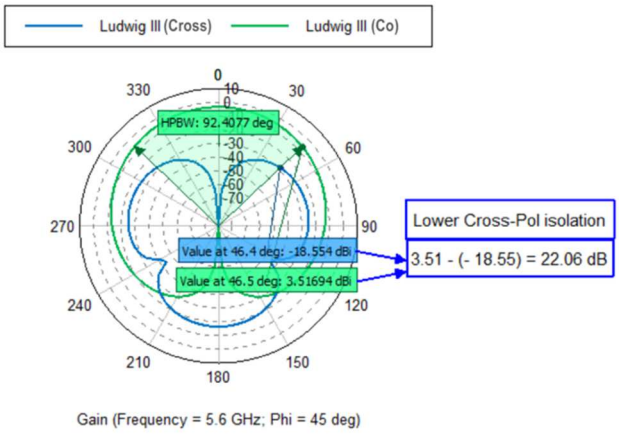

Fig. 15 - Isolation between co and cross-polarization (Freq.: 5.6 GHz).

VII. Conclusions

We present a design of an antenna that can be used for two frequency bands, mainly designed for weather radar bands, which can be used with any polarization, with good characteristics in regards to matching ports, cross-pol isolation, and radiation pattern. Indeed, this design could be used as a basic radiator in an array or as a feeder for a reflector. In summary, the present design achieves the initial objectives proposed.

VIII. References

[1] J. George and V. Chandrasekar, "Front-X phased array weather radar test bed," in *2016 IEEE International Symposium on Phased Array Systems and Technology (PAST)*, Oct. 2016, pp. 1–7. doi: 10.1109/ARRAY.2016.7832547.

[2] H. Saeidi-Manesh and G. Zhang, "Dual-Polarized Aperture-Coupled Hybrid-Fed Microstrip Patch Antenna for MPAR Application," in *2018 IEEE International Symposium on Antennas and Propagation USNC/URSI National Radio Science Meeting*, Jul. 2018, pp. 2141–2142. doi: 10.1109/APUSNCURSINRSM.2018.8608351.

[3] C. F. Castillo-Rubio and J. M. Pascual, "Current Full Digital Phased-Array Radar developments for Naval applications," in *2019 IEEE International Symposium on Phased Array System Technology (PAST)*, Oct. 2019, pp. 1–6. doi: 10.1109/PAST43306.2019.9021011.

[4] S. Karimkashi *et al.*, "Cylindrical polarimetric phased array radar demonstrator: Design and analysis of a frequency scanning antenna array," in *2013 IEEE International Symposium on Phased Array Systems and Technology*, Oct. 2013, pp. 477–480. doi: 10.1109/ARRAY.2013.6731874.

[5] "UIT - Use of Radio Spectrum for Meteorology: Weather, Water and Climate Monitoring and Prediction."

[6] C. R. Peñafiel-Ojeda, M. Cabedo-Fabrés, E. Antonino-Daviu, and M. Ferrando-Bataller, "Design of an unidirectional UWB cavity backed antenna," in *2017 IEEE MTT-S International Conference on Numerical Electromagnetic and Multiphysics Modeling and Optimization for RF, Microwave, and Terahertz Applications (NEMO)*, May 2017, pp. 28–30. doi: 10.1109/NEMO.2017.7964176.

[7] C. R. Peñafiel-Ojeda, A. Llanga-Vargas, M. Cabedo-Fabrés, and M. Ferrando-Bataller, "Elliptical Disk Cavity Backed Antenna for UWB Systems," in *2019 IEEE International Symposium on Antennas and Propagation and USNC-URSI Radio Science Meeting*, Jul. 2019, pp. 1101–1102. doi: 10.1109/APUSNCURSINRSM.2019.8889316.

[8] R. Martens, E. Safin, and D. Manteuffel, "Inductive and capacitive excitation of the characteristic modes of small terminals," in *2011 Loughborough Antennas Propagation Conference*, Nov. 2011, pp. 1–4. doi: 10.1109/LAPC.2011.6114141.

[9] R. Garbacz and R. Turpin, "A generalized expansion for radiated and scattered fields," *IEEE Transactions on Antennas and Propagation*, vol. 19, no. 3, pp. 348–358, May 1971, doi: 10.1109/TAP.1971.1139935.

[10] R. Harrington and J. Mautz, "Computation of characteristic modes for conducting bodies," *IEEE Transactions on Antennas and Propagation*, vol. 19, no. 5, pp. 629–639, Sep. 1971, doi: 10.1109/TAP.1971.1139990.

[11] R. Harrington and J. Mautz, "Theory of characteristic modes for conducting bodies," *IEEE Transactions on Antennas and Propagation*, vol. 19, no. 5, pp. 622–628, Sep. 1971, doi: 10.1109/TAP.1971.1139999.

[12] J. P. Ciafardini, E. A. Daviu, M. C. Fabrés, N. M. Mohamed-Hicho, J. A. Bava, and M. F. Bataller, "Crossed-slot antenna array design for an Incoherent Scatter Radar and characteristic modes analysis," in *2016 10th European Conference on Antennas and Propagation (EuCAP)*, Apr. 2016, pp. 1–5. doi: 10.1109/EuCAP.2016.7481131.

[13] M. Vogel, G. Gampala, D. Ludick, U. Jakobus, and C. J. Reddy, "Characteristic Mode Analysis: Putting Physics back into Simulation," *IEEE Antennas and Propagation Magazine*, vol. 57, no. 2, pp. 307–317, Apr. 2015, doi: 10.1109/MAP.2015.2414670.

[14] A. F. Peterson, S. L. Ray, and R. Mittra, *Computational Methods for Electromagnetics*, 1st edition. New York : Oxford: Wiley-IEEE Press, 1997.

[15] E. K. Miller and L. Medgyesi-Mitschang, *Computational Electromagnetics: Frequency-Domain Method of Moments*. New York: IEEE, 1992.

[16] B. B. Q. Elias, P. J. Soh, A. A. Al-Hadi, P. Akkaraekthalin, and G. A. E. Vandenbosch, "A Review of Antenna Analysis Using Characteristic Modes," *IEEE Access*, vol. 9, pp. 98833–98862, 2021, doi: 10.1109/ACCESS.2021.3095422.

[17] M. Cabedo-Fabres, A. Valero-Nogueira, E. Antonino-Daviu, and M. Ferrando-Bataller, "Modal analysis of a radiating slotted PCB for mobile handsets," in *2006 First European Conference on Antennas and Propagation*, Nov. 2006, pp. 1–6. doi: 10.1109/EUCAP.2006.4584647.

[18] "Electromagnetic Simulation Software | Altair Feko." https://altairhyperworks.com/product/FEKO (accessed Aug. 29, 2020).

[19] J. P. Ciafardini, E. A. Daviu, M. C. Fabrés, N. M. Mohamed-Hicho, J. A. Bava, and M. F. Bataller, "Analysis of crossed dipole to obtain circular polarization applying Characteristic Modes techniques," in *2016 IEEE Biennial Congress of Argentina (ARGENCON)*, Jun. 2016, pp. 1–5. doi: 10.1109/ARGENCON.2016.7585266.

[20] A. Ludwig, "The definition of cross polarization," *IEEE Transactions on Antennas and Propagation*, vol. 21, no. 1, pp. 116–119, Jan. 1973, doi: 10.1109/TAP.1973.1140406.